Proceedings of the International Symposium on Engineering Lessons Learned from
the 2011 Great East Japan Earthquake, March 1-4, 2012, Tokyo, Japan

STRUCTURAL ASSESSMENT OF A REPAIRED CABLE BRIDGE DAMAGED IN 1999 CHI-CHI EARTHQUAKE

Kuo-Chun CHANG[1], Zheng-Kuan LEE[2] and Chien-Chou CHEN[3]

[1] Director, National Center for Research on Earthquake Engineering
Taipei, Taiwan, kcchang@ncree.narl.org.tw
[2] Associate Research Fellow, National Center for Research on Earthquake Engineering
Taipei, Taiwan, zklee@ncree.narl.org.tw
[3]Professor, Yunlin University of Science and Technology
Yulin, Taiwan,ccchen@ce.yuntech.edu.tw

ABSTRACT: The Chi-Lu cable-stayed bridge was damaged during Chi-Chi Earthquake just before completion of its construction. Urgent repairs were made following the earthquake without having made a detailed assessment of the damaged structure. To assess the structural safety, a series of field tests were implemented, including load tests, ambient vibration test and forced vibration test. This paper presents the assessments on the structural safety of the bridge by field tests before the official re-opening, and the health monitoring of this bridge since its reopening to general traffic conditions.

Key Words: Chi-Chi Earthquake, cable-stayed bridge, cable force, wind/rain cable vibration, bridge health monitoring, optic-fiber sensor

INTRODUCTION

Chi-Lu Cable-Stayed Bridge, located at central Taiwan, crossing Juosheui River and linking north Chi-Chi Township and south Lu-Ku Village, is a modern design pre-stressed concrete cable-stayed bridge. As shown in Fig.1, the bridge is composed of a single pylon (58 meters height above the deck), two-row fanned cables (68 cables), and a streamline-shape main girder (2.75 meters in depth and 24 meters in width). The girder rigidly connects the pylon with spans 120 meters to each side bent. On September 21, 1999, during the final construction stage of the bridge, Chi-Chi Earthquake with 7.3 ML magnitude seriously struck central Taiwan. Fig.2 shows the fault line and the bridge's location. Fourteen kilometers away from the epicenter, the nearby Sun Moon Lake Strong Motion Station reveals 989 gal in East-West direction and 423 gal in North-South direction. Chi-Lu Bridge experienced the near-fault strong ground motion, much greater than its seismic design 0.28 G (Chang et al. 2004). After two-stage repair, following the re-opening of the bridge, a FBG based structural monitoring system has been implemented to the structure to monitor the structural behavior of the bridge during routine operation. Based on the field observation and experiments from the last few years, this paper briefly describes the damage, the repair process, the loading tests, and the long-term structural monitoring system on Chi-Lu Cable-Stayed Bridge.

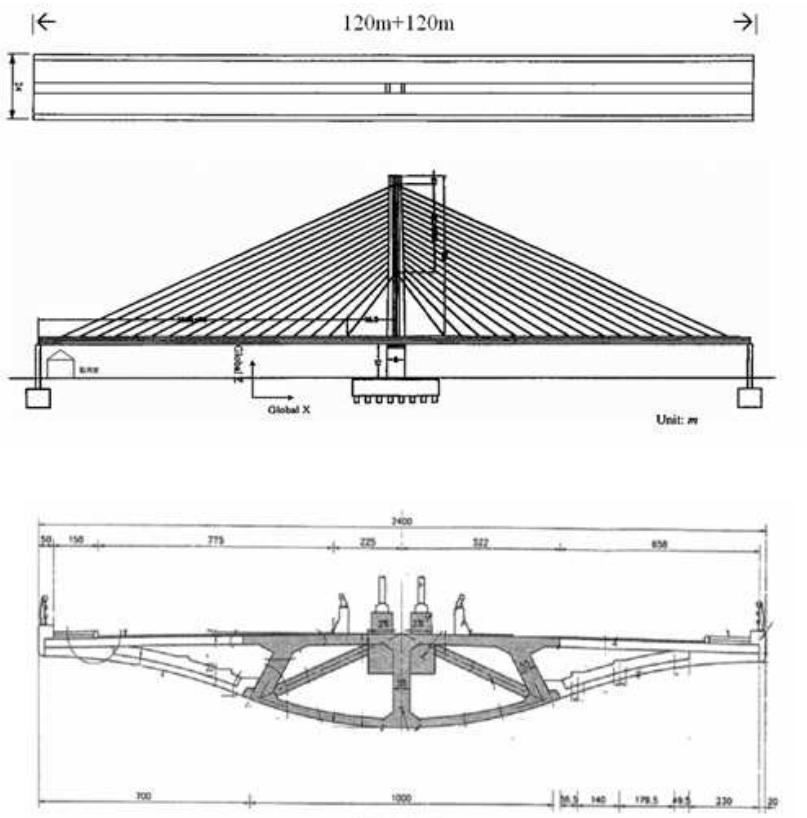

Fig. 1 Profile of Chi-Lu Cable-Stayed Bridge

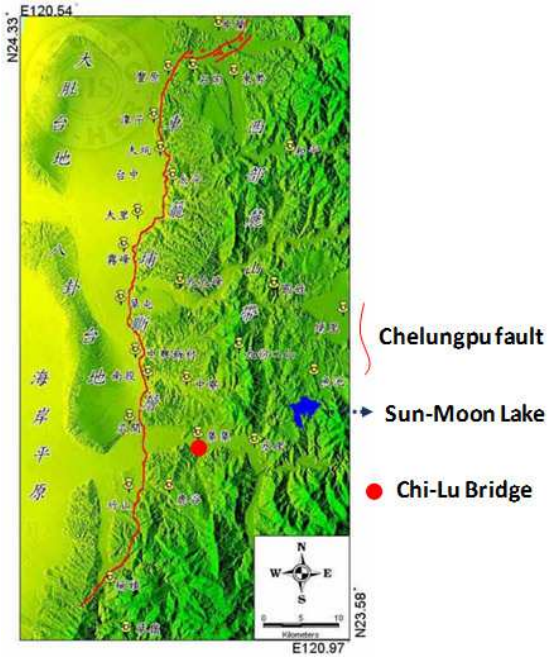

Fig. 2 Map of Chelungpu fault, Chi-Lu Bridge, and Sun-Moon Lake

DAMAGE AND EMERGENT TREATMENT

Shaken by Chi-Chi Earthquake, the Chi-Lu Cable-Stayed Bridge was known as the first damaged modern prestressed-concrete cable-stayed bridge. The observed damage is as follows. The protective concrete cover of the pylon spalled (Fig.3a); one cable fell onto the deck (Fig.3b); the soffit of the girder at the juncture with the pylon cracked (Fig.3c); the rebar in the transverse direction of the girder buckled in compression (Fig.3d); the cap beams of the two bents were damaged by the vertical and lateral pounding forces (Fig.3e); the eccentric device of the guide pipes come off (Fig.3f); and the elevation profile of the deck was lower than that of the design profile (Fig.4). For preventing further damage from more earthquakes, 18 supporting frames were set up (Fig.5) before completion of the repair.

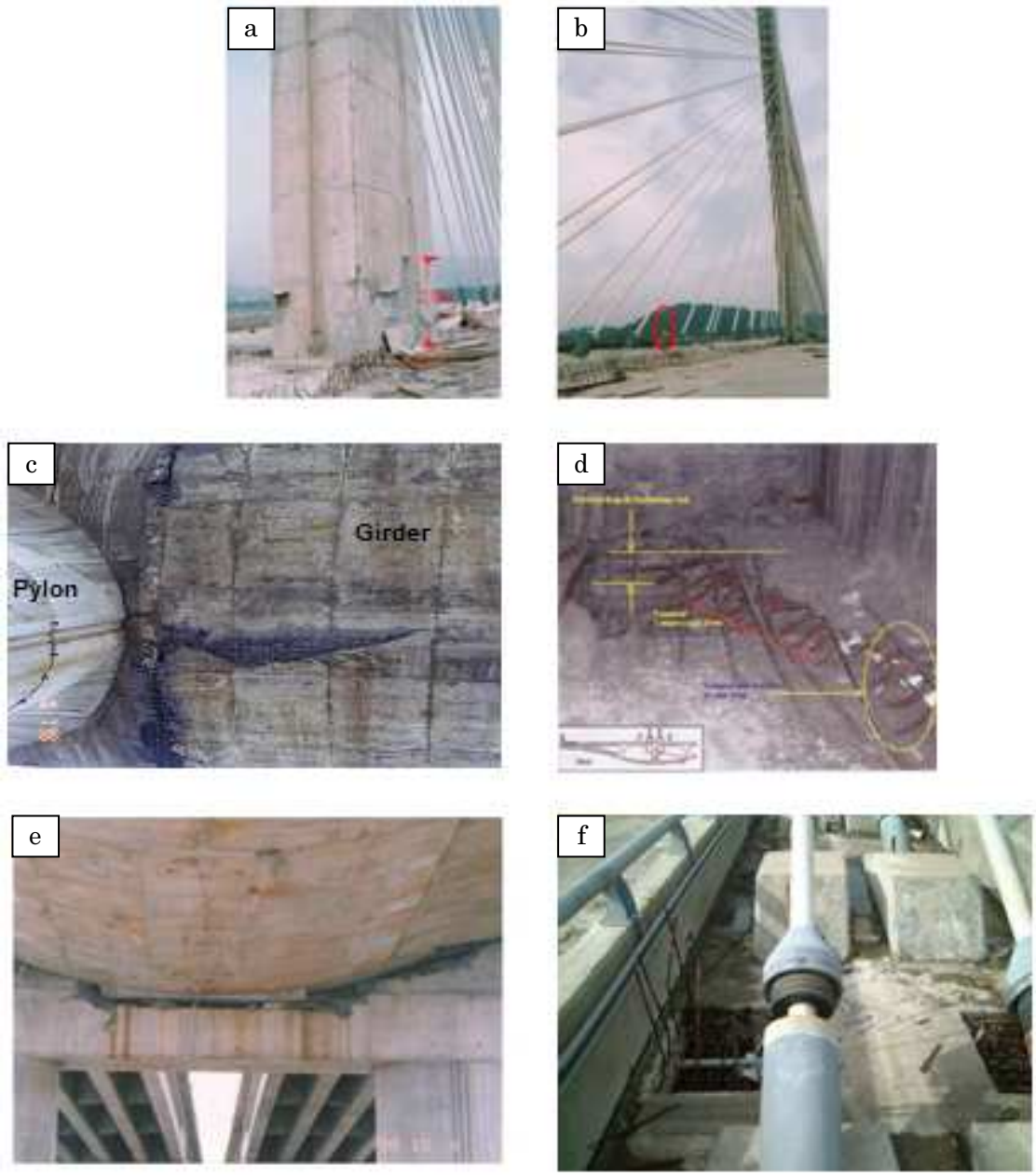

Fig. 3 Chi-Lu Cable-Stayed Bridge damage after Chi-Chi Earthquake

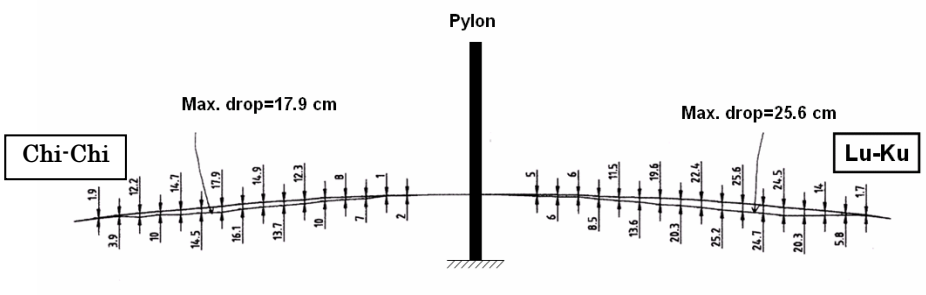

Fig. 4 Elevation profile of the deck after the earthquake

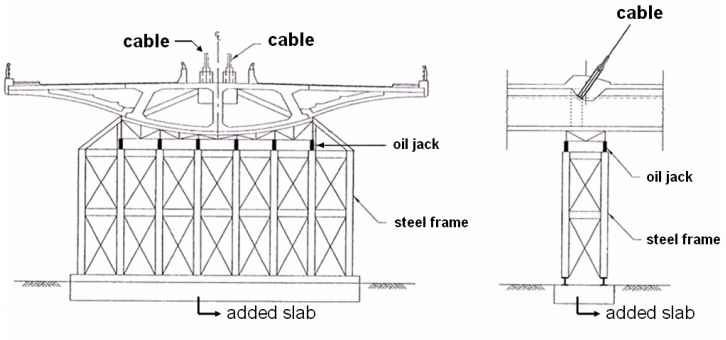

Fig. 5 One of the 18 supporting frames

REPAIR OF THE DAMAGE

Chi-Lu Bridge was unexpectedly damaged by the quake during its final construction stage. The related engineering lawsuit delayed the repair schedule, and the repair process was implemented in two stages. Stage 1: All reinforced concrete components were repaired by July 2001. Stage 2: The cable system was repaired by August 2004. Fig.6 shows the repair of the girder near the pylon. Fig.7 shows the repair of the bent. Fig.8 shows a cable with a new anchor was hanged from the deck to the pylon, and the cable force was being tensioned.

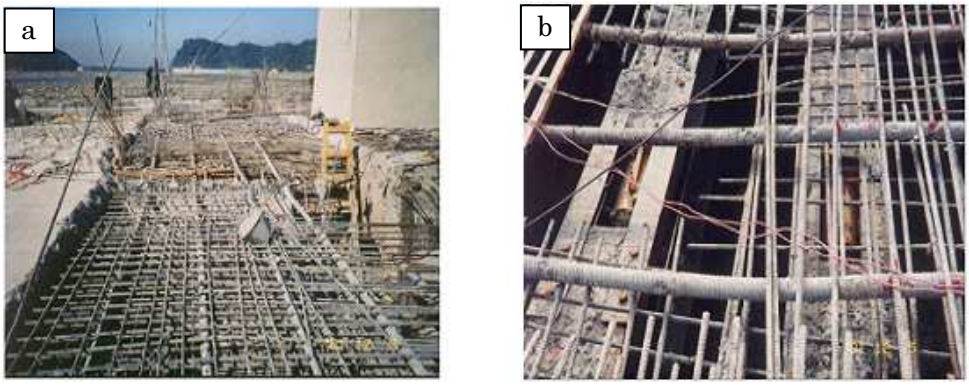

Fig.6 Repair of the girder near the pylon: (a) new rebar mesh, (b) hydraulic jacks inside the girder to balance the compressive force

Fig. 7 New cap beam reconstruction

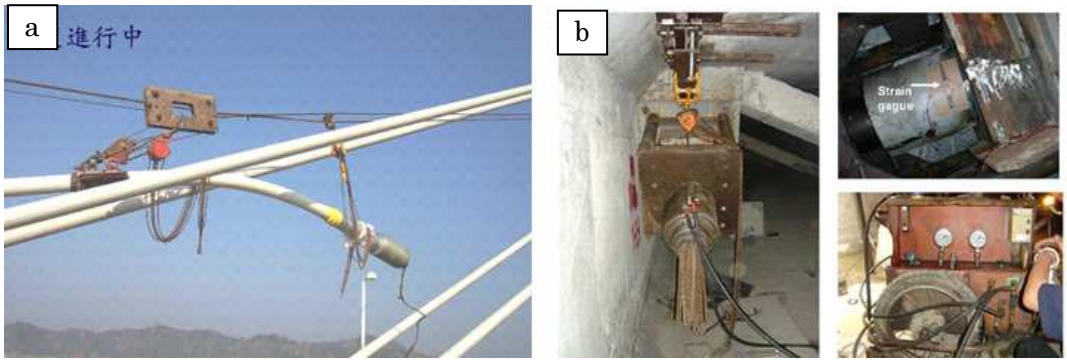

Fig.8 Repair of the cable system：(a) a cable with new anchor was hanged to the pylon, (b) the cable force was measured and tensioned inside the girder

SAFETY LOADING TESTS ON THE DECK

After Repair Stage 1, to partially relieve the traffic demand, the bridge owner entrusted NCREE (National Center for Research on Earthquake Engineering) with the 1st truck loading test, as shown in Fig.9. After the 1st loading test, Chi-Lu Bridge was opened to passersby and passenger cars only.

After Repair Stage 2, the bridge owner entrusted NCREE for the 2nd truck loading test. After the 2nd loading test, as shown in Fig.10, Chi-Lu Bridge was officially opened to the general traffic. During the 2nd loading test, to measure the response of the girder and pylon, both LVDT and tilt meter were deployed as shown in Fig.11. The LVDT were installed on the top of the scaffoldings, setup above the riverbed. Two critical loading patterns were applied on the deck. One is the two-span loading, and the other is single-span loading, as shown in Fig.10a and Fig.10b, respectively. Table 1 lists both the experimental results and the numerical results by the FEM model used the original design. In the two-span loading pattern, the displacement response is close to that of the design value; in the single-span loading pattern, the displacement response is more conservative than the design value. After the loading test that ensured the safety of the bridge, Chi-Lu Bridge then was officially opened to the general traffic.

Fig.9 The 1st loading test after Repair Stage 1

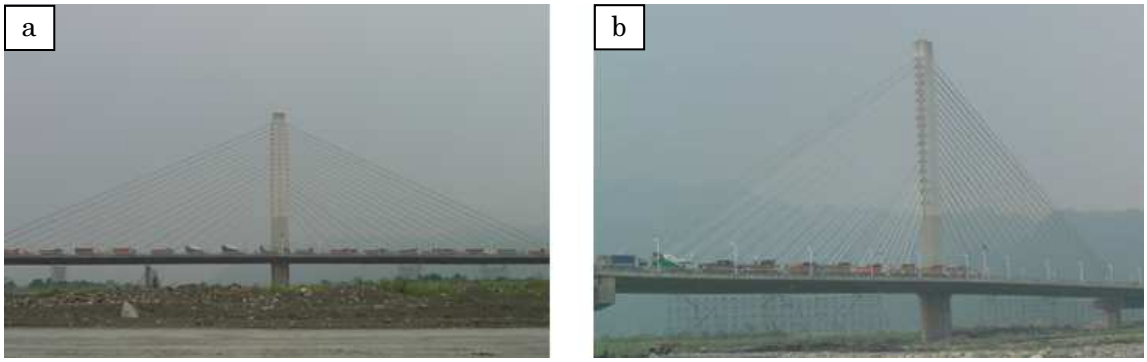

Fig.10 The 2nd loading test after Repair Stage 2

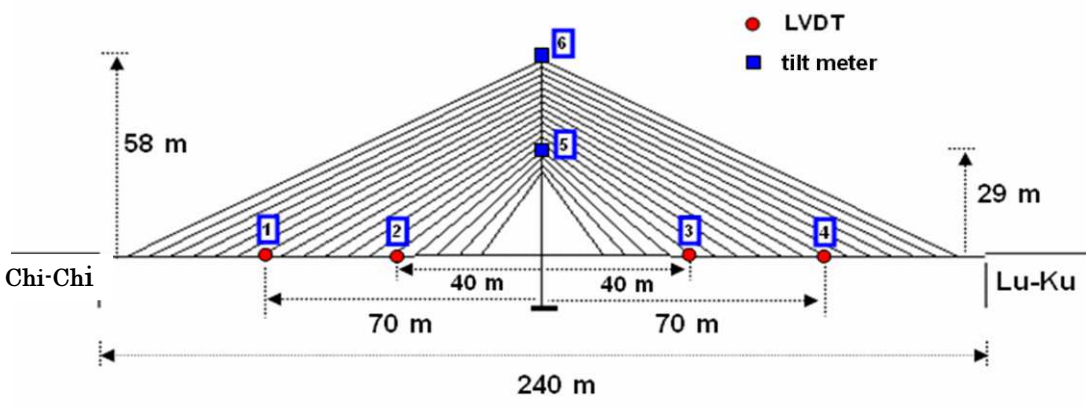

Fig.11 Sensor deployment for the 2nd loading test

Table 1 Comparison between the experiment result and the design analysis

	Channel	Two-span loading Experiment /Design	Single-span loading Experiment /Design
Displacement	1	4.0 cm / 3.7 cm (↓)	7.4 cm / 9.3 cm (↓)
	2	2.0 cm / 2.0 cm (↓)	5.2 cm / 6.3 cm (↓)
	3	1.8 cm /2.0 cm (↓)	3.6 cm / 4.3 cm (↑)
	4	3.9 cm / 3.7 cm (↓)	5.3 cm / 5.7 cm (↑)
Slope	5	0.0013° / 0 (+)	0.0405° / 0.0436° (+)
	6	0.0009° / 0 (+)	0.0161° / 0.0113° (+)

LOADING TEST ON CABLES

During the Repair Stage 2, the cables were replaced. The cable forces and cable vibrations were measured simultaneously by hydraulic jacks (Fig.8b) and velocity-meters (Fig.12a) respectively. The identified cable forces by FEM analysis together with the velocity spectrum were compared with those measured by the hydraulic jacks.

Consider the example of Cable R33, one of the four longest cables of this bridge. Fig.12b shows the measured velocity spectrum with 23 characteristic frequencies. On the other hand in the FEM analysis, a beam model subjected to gravity and geometry-nonlinearity was adopted. The parameters to be determined are the cable force and the moment inertia. After the optimization process, the identified cable force is 1.66E6 N, and the moment inertia is 5.0E-6 m^4. Table 2 compares the characteristic frequencies from the measured and those from the analysis. The analyzed cable sag, shown in Fig.13, is 49.0 cm.

To verify the analyzed cable sag value, two surveyors measured the sag. From the survey, the sag is 50.0 cm, which is close to 49.0 cm. To verify the identified cable force 1.66E6 N, the hydraulic jack in Fig.8b read the cable force 1.69E6 N, which is also closed to the identified cable force1.66E6 N. Without applying formulas, and not knowing the sag and the moment inertia in advance, the identified results yield good agreements with the surveyed sags as well as those measured cable forces. With the identified sag and the identified moment inertia, and the measured frequencies, by practical formulas (Zui H. et al. 1996), one can check on the cable force.

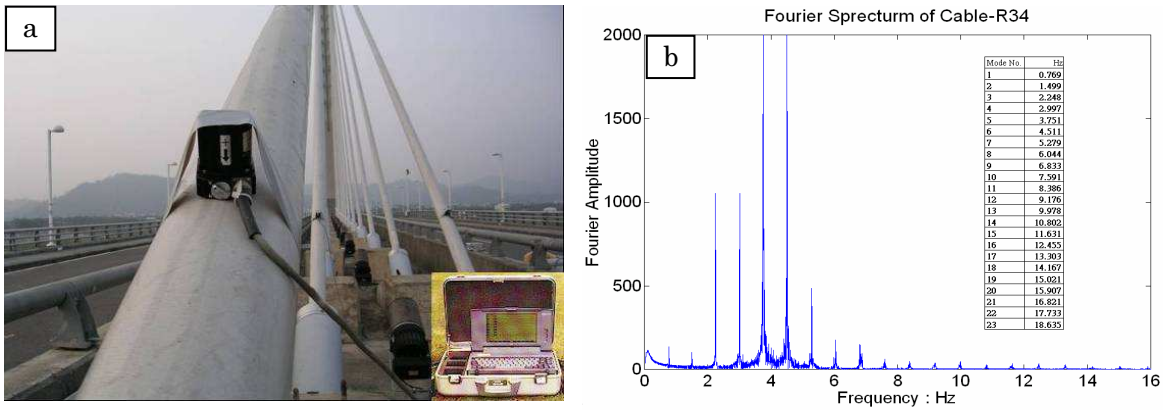

Fig.12 Cable vibration measurement and its signal spectrum

Table 2 Characteristic frequency comparison between the measured and the identified

Mode Number	Measured (Hz)	Identified (Hz)
1	0.769	0.769
2	1.499	1.496
3	2.248	2.247
4	2.997	2.999
5	3.751	3.755
6	4.511	4.514
7	5.279	5.278
8	6.044	6.047
9	6.833	6.822
10	7.591	7.604
11	8.386	8.393
12	9.176	9.190

Mode Number	Measured (Hz)	Identified (Hz)
13	9.978	9.996
14	10.802	10.81
15	11.631	11.63
16	12.455	12.47
17	13.303	13.32
18	14.167	14.18
19	15.021	15.05
20	15.907	15.93
21	16.821	16.83
22	17.733	17.74
23	18.635	18.67

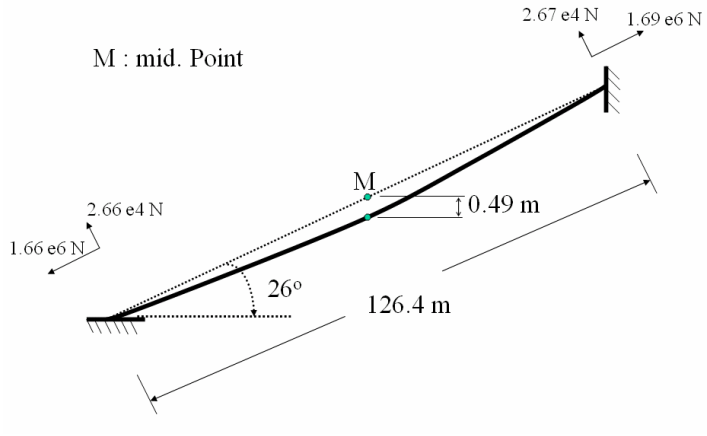

Fig.13 The identified cable configuration with sag 49 cm

FBG-BASED LEVEL SENSORS

After opening to the general traffic, the bridge is concerned with its routine performance. Therefore, to survey the level of the deck is necessary for the bridge management. Instead of manually operating a theodolite, FBG-based level sensors were applied to monitor the level of the girder. The level sensor is a device used to measure the change in elevation between points by using the connected pipe principle, the buoyancy principle, and Hooke's Law of the Fiber Bragg Grating. Fig.14 illustrates how it works (Carlos et al. 2011, and Halliday et al. 1997).

The level sensors were placed inside the girder, shown in Fig.15, where P3 and P4 were immediately beside the pylon and serve as reference points. Beginning at noon one day, and ending at noon the next day, the girder elevation was continually monitored for 24 hours in Fig.16. At 5:00 pm, the bridge temperature peaked, the steel cables lengthened, and P2 and P5 elevations decreased, whereas between 3:00 am and 8:00 am, the bridge temperature was the lowest, the steel cables contracted, and P2 and P5 elevation increased.

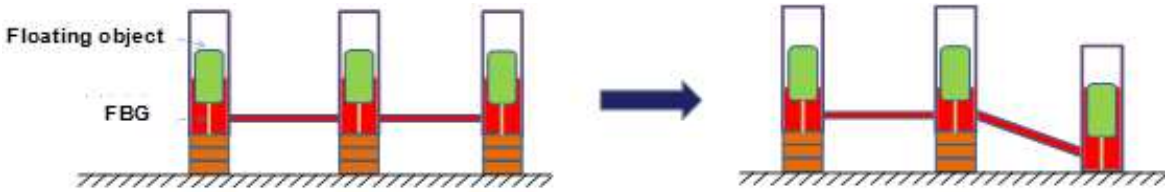

Fig.14 FBG-based level sensor

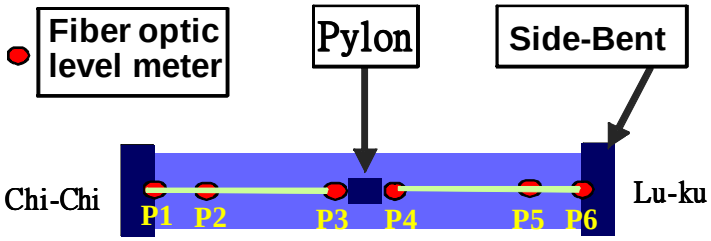

Fig.15 Deployment of FBG-based level sensors

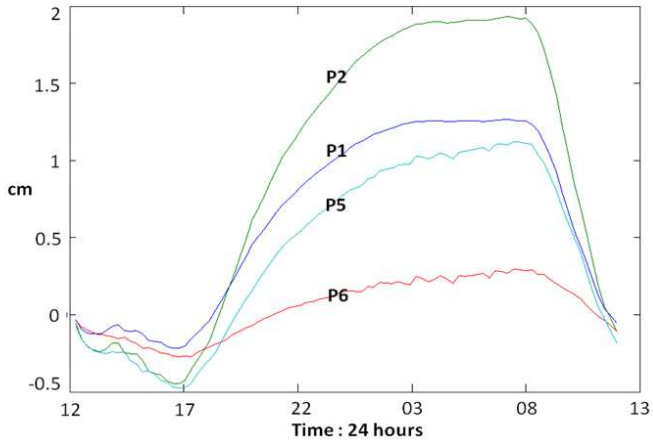

Fig.16 Monitoring the level change for 24 hours

Furthermore, to observe the elevation change induced by traffic, the quasi-static signal in Fig.16 could be filtered out. As shown in Fig. 17, two trucks drove onto the deck at different time. The truck that first arrived had driven from Chi-Chi; thus, P1 and P2 simultaneously dropped and P5 and P6 simultaneously rose. When the truck passed the pylon and crossed over onto the Lu-Ku end, P1 and P2 increased to their original positions and P5 and P6 dropped simultaneously. When the truck left the bridge, the girder returned to its original stable level. About 200 s later, the second truck drove over the bridge from Lu-Ku. The change in the girder's elevation was similar to that under the first truck, only the order and timing of the dropping and rising was reversed. It is demonstrated that the FBG-based level sensors can trace the girder level influenced by temperature change and traffic loading. From the regular observation, the girder level is stable without obvious settlement since the bridge's opening to the general traffic.

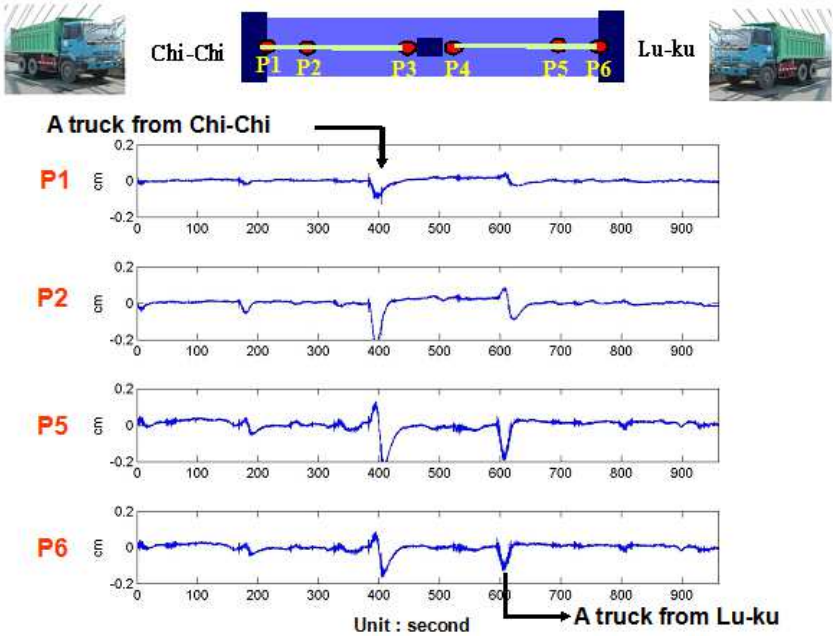

Fig.17 Vertical response to two trucks

FBG-BASED VIBRATION SENSORS FOR CABLES

Cable forces compose an important health index of a cable-stayed bridge. For evaluating the cable forces, conventionally, electric sensors are attached on cables to measure the vibration. As shown in Fig.12a, through electric wires, sensors are parallel connected to the datalog. With limited expensive sensors and channels, to permanently measure all 68 cables simultaneously becomes very difficult if not impossible. Besides the economic factor, lightening and rain are hazardous to electric instruments.

To overcome the difficulties mentioned above, self-assembled FBG vibration sensors are installed on the cables as illustrated in Fig.18. One optic channel measures 17 cables, and only four channels are required for the 68 cables. Through the Internet, the cable vibration spectrum are automatically analyzed and reported back. By this way, all cable forces can be evaluated simultaneously without routine manual labor works. From the measured data, all cable forces are considered to be normal since the bridge's re-opening to the general traffic.

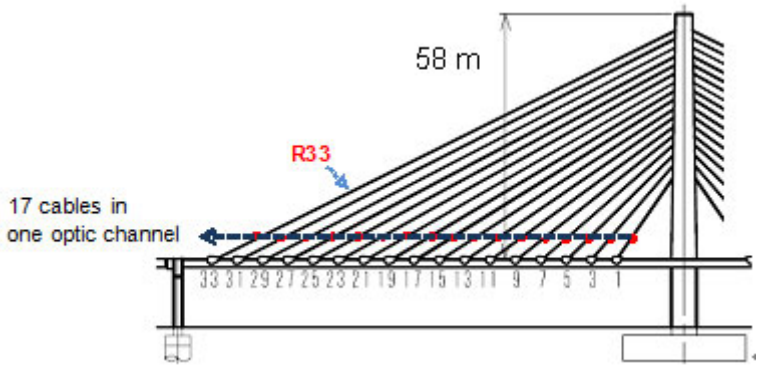

Fig.18 One optic channel measuring 17 cables' vibration

WIND/RAIN CABLE VIBRATION

Geographically, Taiwan is constantly suffering the threat of both earthquakes and typhoons. Typhoons bring torrential and strong wind, cause floods to damage bridges, and probably induce the wind/rain cable vibration on cable-stayed bridges. With the FBG vibration sensors for cables, the wind/rain cable vibration of Chi-Lu Bridge had been measured and video-taped.

On July 28, 2008, Fung-Wong Typhoon went across Taiwan. Fig.19 shows the vibration spectrum of Cable R33 before and during the wind/rain vibration. From Fig.19, the vibration spectrum before the wind/rain vibration was distributed along each mode, but was more concentrated and stronger on the second mode during the wind/rain vibration. Besides, the strong cable vibration was also video-taped. The field observation demonstrates that some cables of Chi-Lu Cable-Stayed Bridge may behave in wind/rain instability.

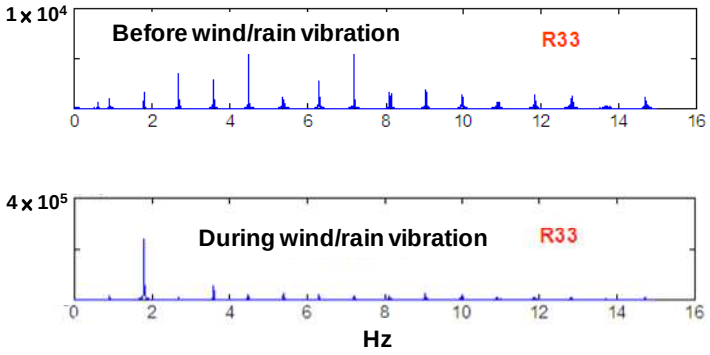

Fig.19 Spectrum comparison before and during wind/rain vibration

To further study the inherent cable damping (Pacheco, B. et al. 1993), a pull-and-release experiment, as shown in Fig. 20, was carried out to determine the damping ratio and the Scruton Number:

$$Sc = \frac{m\xi}{\rho D^2} \tag{1}$$

Where m is the mass per unit length, ξ is the damping ratio, ρ is the air density, and D is the cable diameter. Table 3 lists the Scruton Number for three cables. According to PTI (1993), if the Scruton Number is less than 1.7, wind/rain induced vibration will readily occur. The measured wind/rain vibration signal, the taped video, and the pull-and-release experiment agree with the PTI recommendations.

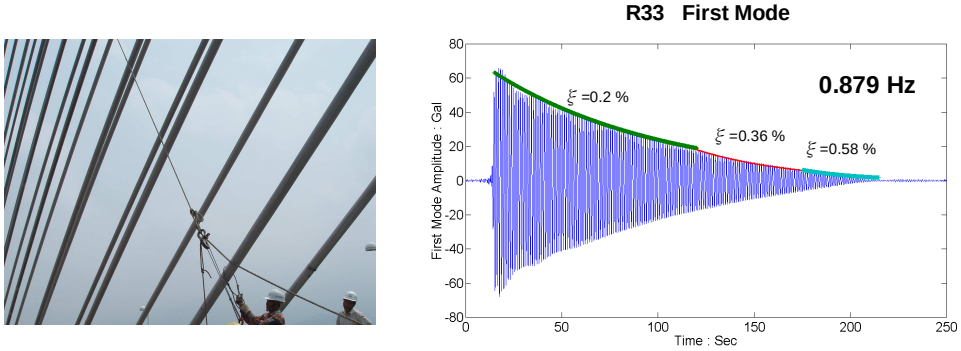

Fig.20 The pull-and-release forced vibration and the damping analysis

Table 3 Scruton Number for the first three modes of three cables

Mode	R33	R31	R29
1st	1.86	2.72	3.31
2nd	1.12	2.96	2.60
3rd	1.21	2.96	1.89

CONCLUSIONS

Because of Chi-Chi Earthquake, Chi-Lu Cable-Stayed Bridge performs as a rare but valuable example for research on cable-stayed bridges about the near-fault strike, damage patterns, emergent treatments, repair processes, safety loading tests before re-opening, and the long-term structural monitoring. The following summarizes this study.

(1) About the girder, loading test on the deck was performed and analyzed. In addition, FBG-based level sensors are installed and demonstrated effective to temperature change and traffic loading.
(2) About the cables, loading test、force evaluation、wind/rain instability observation during typhoon、pull-and-release test, and FBG-based sensors for all 68 cables, etc., were carried out and analyzed.
(3) From the regular measurements, the cable system and the deck elevation are normal since opening. However, some long cables may be insufficient to wind/rain stability.
(4) To reduce routine labor work in survey, FBG-based sensors are self-assembled and installed on the bridge. It's demonstrated that FBG sensors have substantial potential for monitoring cable-stayed bridges.

ACKNOWLEDGMENTS

The authors wish to express their thanks to Directorate General of Highways, MOTC for the research funding and the field experiment assistance on Chi-Lu Cable-Stayed Bridge.

REFERENCES

Carlos, R., Carlos, F., and Joaquim, F. (2011). "Fiber-optic-based displacement transducer to measure bridge deflections," *Structural Health Monitoring*, Vol. 10, No. 2, 147-156.

Chang K. C., Mo Y. L., Chen C. C., Lai L. C., and Chou C. C. (2004), "Lessons learned from the damaged Chi-Lu Cable-Stayed Bridge", *Journal of Bridge Engineering*, ASCE, Vol.9, No.4, 343-352.

Halliday, D., Resnick, R. and Walker, J. (1997). "Fundamentals of Physics," Wiley Interscience Publications, New York, USA.

Pacheco, B., Fujino, Y. and Suelk, A. (1993). "Estimation curve for modal damping in stay cables with viscous damper," *Journal of Structural Engineering*, ASCE, Vol.119, No. 6, 1961-1979.

Post-Tensioning Institute Committee on Cable-stayed Bridges (1993) "Recommendations for stay cable design, testing, and installation."

Zui H., Shinke T., and Namita Y. (1996), "Practical formulas for estimation of cable tension by vibration method," *Journal of Structural Engineering*, ASCE, Vol.122, No. 6, 651-656.